Validity of common assumptions for anomalous scattering

John C. Parker and R. H. Pratt
Department of Physics and Astronomy, University of Pittsburgh, Pittsburgh, Pennsylvania 15260
(Received 28 February 1983)

The usual description of Rayleigh scattering (the component of elastic photon-atom scattering identified with scattering from bound electrons) separates the high-energy fixed-momentum-transfer limit (generally taken to be specified in terms of the atomic form factor) from additional contributions to the amplitude, known as anomalous scattering factors or anomalous dispersion corrections. We use explicit results from a full relativistic numerical calculation of Rayleigh scattering to emphasize that several common assumptions regarding these anomalous scattering factors, still mistakenly used although previously criticized, are not entirely appropriate: (1) The anomalous scattering factors should not be identified with the difference from form factor; (2) the imaginary forward scattering factor f'' is not determined solely from photoeffect at high energy ($\gtrsim 2mc^2$); (3) the imaginary forward amplitude includes bound-bound resonance contributions below the photoeffect threshold, which are needed to ensure that the real forward scattering factor obtained from f'' through a dispersion relation goes to a finite value as the threshold is approached from above; (4) the imaginary anomalous amplitudes do not have the angular dependence of the form factor, but rather a weaker angular dependence, with the consequence that the imaginary amplitude can be comparable in magnitude with the real amplitude at some nonforward angles; and (5) the ratio of parallel and perpendicular anomalous amplitudes is not simply $\cos\theta$.

I. INTRODUCTION

In this paper we use results obtained from our procedures[1] for relativistic numerical evaluation of Rayleigh scattering in partial waves to examine the validity of assumptions often made in the description of anomalous scattering of photons from atoms. This work discusses the atomic scattering factor f which characterizes the anomalous effects due to electron binding in the scattering from an isolated atom; $|f|^2$ must for example be multiplied by a structure function to obtain the intensity of scattering from a crystalline sample. Our calculation of Rayleigh scattering (the contribution to elastic photon-atom scattering due to scattering from the bound-atomic electrons) describes the matrix element as the coherent sum of second-order S matrix elements for photon scattering from electrons bound in a relativistic screened self-consistent central potential. This approach, which neglects correlation and exchange (beyond a local Slater exchange term), is expected to be sufficient except within some tens of eV of a threshold. In obtaining cross sections a constant nuclear Thomson amplitude is added, which becomes significant for larger momentum transfers. Generally satisfactory agreement has been achieved with experimental studies of x-ray[1] and γ-ray[1,2] scattering from atoms, representing an improvement upon previous numerical[3–7] and analytic[8–10] calculations. Here we focus our attention on the energy and momentum-transfer dependence of the scattering factor above and below the K-threshold region, looking both at a light-Z element (aluminum) and a high-Z element (lead).

By anomalous scattering, early studied by the x-ray crystallographers,[11–13] is meant the rapid variation of scattering cross sections at energies near (both above and below) regions of atomic excitation and ionization threshold, resulting in "anomalous" behavior of the x-ray index of refraction. Anomalous scattering factors may be defined in terms of the difference from the (constant) scattering amplitudes found far above threshold and, if so defined, in the forward direction the real and imaginary parts of such anomalous factors may be related through dispersion relations.[12–15] The high-energy limit of the scattering amplitude is often assumed to be determined from the atomic form factor (the Fourier transform of the electron charge distribution, which is real), giving at high energy a forward amplitude proportional to the number of bound atomic electrons. The forward imaginary amplitude, which is the same as the imaginary anomalous scattering factor f'', is often taken as proportional to the total photoelectric cross section from a photon of the given energy off the atom in question[11–14]; the forward real amplitude at the same energy is then determined from these imaginary amplitudes through the dispersion relation.[11–14] The angular dependence of these anomalous amplitudes has sometimes been assumed to be the same as in form-factor approximation, as suggested by a classical argument.[16] We shall demonstrate with our explicit calculations that there are difficulties with all of these assumptions, namely, (1) the identification of the anomalous scattering factors with the difference from form factor, (2) the identification of the forward imaginary amplitude with only atomic photoeffect, (3) the use of only atomic photoeffect in the dispersion relation, (4) the assumption that the perpendicular anomalous scattering factors have the angular dependence of the form factor, and (5) the assumption that that ratio of parallel to perpendicular anomalous scattering factors is given by $\cos\theta$. While these difficulties have been noted at various

times,[9,10,15,17,18] the assumptions continue to be used.[6,14,19,20]

More precisely, the exact Rayleigh amplitude may be written

$$f=\epsilon^*_{2,||}\epsilon_{1,\perp}f_{||}(\omega,\theta)+\epsilon^*_{2,\perp}\epsilon_{1,\perp}f_{\perp}(\omega,\theta)\ , \tag{1}$$

characterized by two complex amplitudes $f_{||},f_{\perp}$ for scattering of a photon of energy $\hbar\omega$ through an angle θ, where ϵ_1 and ϵ_2 are the complex polarization vectors of the initial and final photon, $\epsilon_{||}$ and $\epsilon_{\perp}$ their components parallel and perpendicular to the scattering plane. One may show that

$$f_{||}(\omega,0°)=f_{\perp}(\omega,0°),\quad f_{||}(\omega,180°)=-f_{\perp}(\omega,180°). \tag{2}$$

In form-factor (or dipole) approximation $f_{||}=f_{\perp}\cos\theta$. Anomalous scattering factors (real) f' and f'' are often defined[12,14] through

$$f_{\perp}=f_{\perp}^{ff}+\tilde{f}'+if''\ . \tag{3}$$

As we shall see, this definition[21] is inconsistent with the connection of the forward anomalous scattering factors through a dispersion relation, which is why we have written $\tilde{f}'$ rather than f' in Eq. (3).

In Secs. II and III we will use our numerical data to discuss the properties of the forward real and imaginary scattering amplitudes and in Sec. IV we will use the data to discuss the angular dependence of these amplitudes and the anomalous factors. In the process we shall also note the extent to which nonrelativistic Coulomb dipole results for the K shell,[8] when combined with a modified-form-factor approximation,[22] suffice for a qualitative understanding of the Rayleigh scattering amplitudes.

II. THE FORWARD REAL AMPLITUDE

In Fig. 1 we show the forward real amplitude $f_{\perp}(\omega,0°)=f_{||}(\omega,0°)$ for Al and Pb in units of Z, as a function of photon energy $\hbar\omega$ in units of the K-shell binding energy ϵ_K.[23] We may focus our attention on the following features of the amplitude: (1) high-energy behavior, (2) slight maximum for ω near twice the photoionization threshold, (3) finite drop near threshold, (4) resonance region, and (5) low-energy behavior. Gavrila's nonrelativistic Coulomb dipole calculation for hydrogen[6] explicitly illustrates all these features, which can already be seen in the Kramers-Heisenberg matrix element, giving $f=Z$ at high energies (form-factor value), vanishing at low energy, exhibiting resonances at the $1s$-np dipole bound-bound transition energies, and dropping (though not so much as for Al) to a finite value as threshold is approached from above. The modified form factor, originally suggested by Franz,[22] predicts for the forward amplitude a constant which differs from one by terms of order $(Z\alpha)^2$. The component $g_i(q)$ of the modified form factor due to the charge distribution $\rho_i(r)$ of the ith electron is defined as

$$g_i(q)=\int d^3r\, e^{i\vec{q}\cdot\vec{r}}\frac{mc^2}{E_i-v(r)}\ ,$$

where E_i is the total energy (including rest-mass energy) of the electron.

We see that the high-energy limit of the amplitude f, which serves to define the anomalous scattering factors f' and f'' if they are to be connected through a dispersion relation, differs from the form-factor prediction Z by terms of relative order $(Z\alpha)^2$. If we write

$$f(\omega)\equiv \mathrm{Re}f(\omega=\infty)+f'+if'' \tag{4}$$

then,

$$f'(\omega)=\frac{2}{\pi}\int_0^{\infty}\frac{\omega' f''(\omega')}{\omega'^2-\omega^2}d\omega'\ . \tag{5}$$

In fact, for scattering from each atomic electron the correction is of the order of its binding energy, as is predicted by the modified form factor,[22] in Levinger's estimate of relativistic corrections to the dipole sum rule,[24] in the high-energy limit calculation of Goldberger and Low,[17] and as clearly seen in the work of Florescu and Gavrila.[10] The result is that the correction is of the order of the total binding energy of the atom in comparison to the total rest-mass energy of the atomic electrons. The correction is very small for a light element such as Al, but it is visible at the 1% level in the forward cross section of a high-Z element. The difference from the form-factor value in Pb is primarily due to the differences arising in the scattering from its K-shell electrons, but does also reflect the deviations from the form factor of the high-energy limit for the other electrons. The use of $\tilde{f}'$ rather than f' in Eq. (5) provides an explanation for the systematic discrepancy noted by Creagh[25] between f' calculated from photoeffect and f' measured relative to form factor, since the difference $f'-\tilde{f}'$ of form factor from high-energy limit is larger than f' in the circumstances

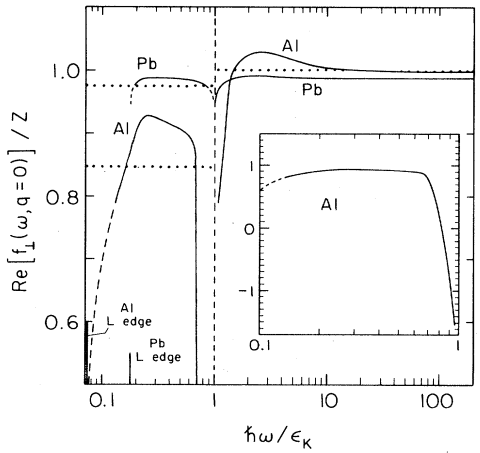

FIG. 1. Forward real amplitudes $Z^{-1}\mathrm{Re}f_{\perp}(\omega,0°)=Z^{-1}\mathrm{Re}f_{||}(\omega,0°)$ in units $\hbar=m_e=c=1$ for Al ($Z=13$) and Pb ($Z=82$) as a function of photon energy $\hbar\omega$ in units of K-shell binding energy ϵ_K (1.510 keV for Al and 87.9 keV for Pb in our model); L edge positions are marked. The solid curve (——) shows our numerical data, the dotted curve (· · · ·) shows the form-factor predictions. Below the K threshold the reduced form-factor value $Z-2$ is shown. The inset shows in detail the approach to a resonance (the $1s$-$3p$ resonance) for Al. Note that $\mathrm{Re}f_{\perp}(\mathrm{Al})=0$ at $(\omega/\epsilon_K)\cong 0.9$, implying a deep minimum in the scattering cross section.

(relatively high energies) of the measurements. Note that this, in principle, affects the interpretation of scattering amplitudes as tabulated by Henke *et al.*,[7] but at low energies where f' is bigger the relative error is much smaller.

Figure 1 shows that the amplitude for scattering from an electron changes little from its high-energy value until the photon energy is only a few times the binding energy, when it exhibits a gentle maximum (rising about 20% in Gavrila's calculation) at a couple of times the binding energy. The rise in the total amplitude above the K threshold is due to the K electrons and so is more noticeable for Al ($\simeq 3\%$) than for Pb ($\lesssim 1\%$), since the K electrons are a greater fraction of the total in a light-Z element. The rise above $Z-2$ in Al above the L threshold is much greater, since most of the electrons in Al are in the L shell and the rise above $Z-2$ in Pb above the L threshold is more visible, again because the electrons are a more significant fraction of the total. The gentle maximum in f' was obtained in calculations with dispersion relations[11–14] using photoeffect results in f'', and it is already predicted in the classical calculation of photon scattering from an electron bound in a harmonic oscillator potential.[26]

The amplitude drops, but to a finite value, as the threshold is approached from above. Gavrila's calculation shows this feature, whereas dispersion relation calculations of f' based on f'' from photoeffect data only instead exhibit a logarithmic divergence.[6,11–14] This divergence is canceled if the contribution to f' from the allowed bound-bound transitions is also included in f''. In Al (in contrast to hydrogen) the $1s$-$2p$ transitions are not allowed (and $1s$-$3p$ is reduced) so that the K-shell amplitude drops further corresponding to the omission of their contribution, and evidently is small at threshold. In fact both for Al and Pb the K amplitude is negative just above the K threshold, so that the total amplitude is less than $Z-2$. At the L edge of Al the drop is even greater.

Between the K threshold and the lowest photoexcitation energy of the very outermost electron, the sequence of subshell thresholds is accompanied by a sequence of resonance regions in scattering (which overlap for outer electrons). In principle the scattering amplitude below each subshell threshold exhibits an infinite sequence of resonances at energies corresponding to allowed bound-bound transitions, as in Gavrila's calculations; this region was not explored in our numerical calculations. These resonances correspond to transitions to unoccupied (excited) states of the atom. In the approximations of our calculations the scattering amplitude will be infinite at the energies corresponding to such bound-bound transitions but if the lifetimes of the excited states are considered the resonances will have finite level widths,[27] with high-lying resonances so broadened and overlapping that they are not observable. Similarly, for an atom in a solid broadening to a continuum with edge-lowering can occur.

Below the K-resonance region photon energies ω become small compared to those needed to excite or ionize a K electron. At such energies the contribution to the total scattering amplitude due to scattering from a K electron decreases monotonically to zero with decreasing energy (as ω^2), as exhibited in Gavrila's calculation.[8] The amplitude in this region is opposite in sign to its value above threshold in the form-factor regime. This means that, except in hydrogen and helium, there is a minimum in the cross section just below the first real resonance of the resonance region (as well as inbetween resonances) as the amplitude (K shell, in this case) cancels the real parts of amplitudes from L shell and higher. This behavior is shown for Al in the inset of Fig. 1. At still lower energy the given electron amplitude is unimportant (if other more lightly bound electrons are present) and the scattering behaves like that for an atom of reduced charge. However, between thresholds the influence of the resonance regions is sufficiently extensive that there are no regions where anomalous effects may be safely ignored, as has long been known.[13] For comparison the dotted lines of Fig. 1 show the reduced form factor values $Z-2$ below the K shell. For energies so low that photoexcitation of the atom is not possible the amplitude will go to zero as ω^2. (At these energies the separation into Rayleigh scattering and nuclear Thomson scattering is not formally valid, but the Rayleigh amplitude alone essentially describes the extreme low-energy regime if the Thomson amplitude is omitted.[28]) The scattering at very low energies from a free atom may be described as scattering from a neutral slightly polarizable target.[4,5]

III. THE FORWARD IMAGINARY AMPLITUDE

In Fig. 2 we show our data for the forward imaginary amplitude in the same circumstances which we have thus far been discussing for the forward real amplitude. According to the optical theorem

$$\mathrm{Im}f(\omega,0)=\frac{\alpha}{4\pi}\frac{\hbar\omega}{mc^2}\frac{\sigma_{\mathrm{abs}}}{(e^2/mc^2)}\equiv\frac{\omega}{4\pi c}\sigma_{\mathrm{abs}}\,, \tag{6}$$

where σ_{abs} is the difference in photoabsorption total cross sections (for transitions involving bound atomic electrons) for a photon incident on an atom and on the corresponding bare atomic nucleus.[15] (Photoabsorption involving pair production of continuum electrons and positrons is

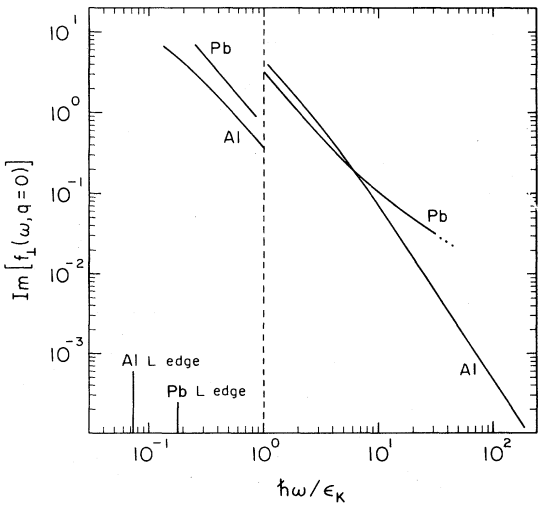

FIG. 2. Forward imaginary amplitudes $\mathrm{Im}f_{\perp}(\omega,0°)$ $[=\mathrm{Im}f_{\parallel}(\omega,0°)]$ for Al and Pb as in Fig. 1.

identified with the Delbruck, rather than with the Rayleigh, amplitude.) We may identify three regions of this amplitude: (1) High energies $\omega \gtrsim 2mc^2$, (2) the photoeffect regime, and (3) the resonance regime.

While σ_{abs} is often taken as the photoeffect cross section, in fact there are two other contributions which are important if correct results are to be obtained when f'' is inserted into a dispersion relation. In the first place, the subtracted photoabsorption cross section on a bare nucleus gives a contribution for $\omega \gtrsim 2mc^2 - \epsilon_K$, ϵ_K the Coulomb K-shell binding energy, corresponding to the possibility of creating an electron-positron pair with the electron bound to the bare atomic nucleus.[15] The high-energy limit[29] of photoeffect is $\sim\omega^{-1}$, so its contribution to Imf tends to a constant and the corresponding integral for the dispersion relation would not exist; this difficulty led to the realization[15] of the existence of the subtracted bound-pair-production term, which has the same high-energy limit as photoeffect. For high energy one then expects a behavior in Imf like $(Z\alpha)^5 mc^2/\hbar\omega \sim (Z\alpha)^3/(\epsilon_K/\hbar\omega)$, which is not yet achieved for the energies shown in our data. (Subtracting the bound-pair creation cross section formally cuts off the dispersion integrals, in effect justifying the cutoff used in numerical calculations of f'.)[6] Secondly, below photoeffect thresholds there will be δ-function (when level widths are not considered) contributions corresponding to real bound-bound radiative transitions. As already noted, these must be included in the dispersion relation if the correct finite threshold limit for f' is to be obtained as threshold is approached from above.

Otherwise, except for the bound-bound transition energies and below the pair-production threshold, Imf is determined from the photoeffect cross sections. In Coulomb dipole approximation the curves as shown should be Z independent, and they do somewhat merge for $\omega \gtrsim \epsilon_K$ but not too large; screening causes larger differences below the K threshold. The amplitudes are dominated by the most deeply bound shell which can be excited. Only as one approaches outer-shell thresholds do magnitudes of Im$f(\omega,0°)$ become comparable with the real amplitudes (in contrast to the finite momentum transfer situation).

IV. THE ANGULAR DEPENDENCE OF ANOMALOUS SCATTERING

We now study the angular dependence (q dependence) of the Rayleigh scattering amplitudes from aluminum (Al) and lead (Pb) near and above the K threshold in the x-ray and soft γ-ray regimes. Here $\hbar q$ is the momentum transfer to the atom in scattering, often expressed in terms of the variable x, where

$$\hbar q = (2\hbar\omega/c)\sin(\theta/2) ,$$

$$q = 4\pi x, \quad x = \lambda^{-1}\sin(\theta/2) ,$$

with θ the scattering angle and λ the wavelength. We will see that even in the circumstances which have been of interest to crystallographers commonly used assumptions regarding the q dependence can fail. We first illustrate the

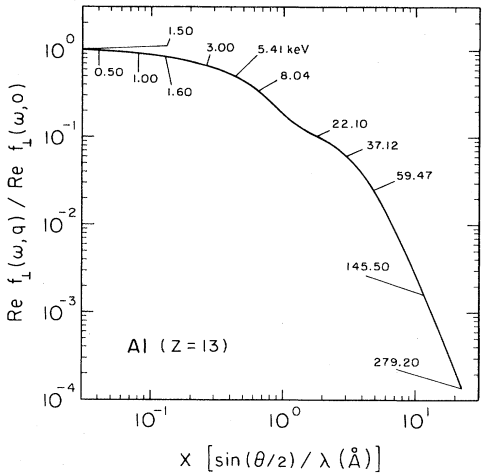

FIG. 3. Momentum dependence of the real perpendicular amplitude normalized to the corresponding forward amplitude, $[\text{Re}f_\perp(\omega,q)]/[\text{Re}f_\perp(\omega,q=0)]$, plotted against momentum transfer $x \equiv \sin(\theta/2)/\lambda$ (Å), for Al at various photon energies as indicated in keV. The solid curve of numerical predictions cannot be distinguished from form factor on this scale. Note that Rayleigh and nuclear Thomson amplitudes are being added to obtain Re$f_\perp$; this has no effect for the Al data shown.

situations for $f_\perp$, which decreases monotonically with q in these ranges and then discuss how the q dependence of $f_{||}$ departs from that predicted by $f_{||} = f_\perp \cos\theta$. (There is a systematic movement of the zero in $f_{||}$ towards angles smaller than 90°.) After studying Re$f_\perp$, Im$f_\perp$, and $f'_\perp$, we will also consider the differential scattering cross section when photon polarization is not observed,

$$\frac{d\sigma}{d\Omega} = \frac{r_0^2}{2}(\,|f_\perp + A_{\text{NT}}|^2 + |f + A_{\text{NT}}\cos\theta|^2) , \tag{7}$$

where $r_0 = e^2/mc^2$ is the classical electron radius and A_{NT} is the nuclear Thomson scattering amplitude. (At higher energies further elastic amplitudes would have to be included to specify the observable elastic scattering process.)

For Al, we show in Fig. 3 the q dependence $|\text{Re}f_\perp(\omega,q)/\text{Re}f_\perp(\omega,0)|$, the real part of $f_\perp$ normalized to its forward direction value for various photon energies $\hbar\omega$ in keV as well as the ω independent form-factor prediction (which is essentially the same as modified form factor in this light Z case). At 1.5 keV the resonance corresponding to a $1s$-$3p$ bound-bound transition is very close (see inset of Fig. 1). It results in a large enhancement of the electric dipole contribution which is independent of angle; consequently the scattering amplitude is anomalously flat. Otherwise, the form factor gives a good prediction for the q dependence of the amplitude at all energies considered. For larger q (at higher energies) the form factor will eventually fail, but the expectation is that at such high q's the nuclear Thomson amplitude (and others) small in the forward direction, will by far dominate over the Rayleigh amplitude contribution to elastic scattering.

However, for high-Z elements form factor fails badly,

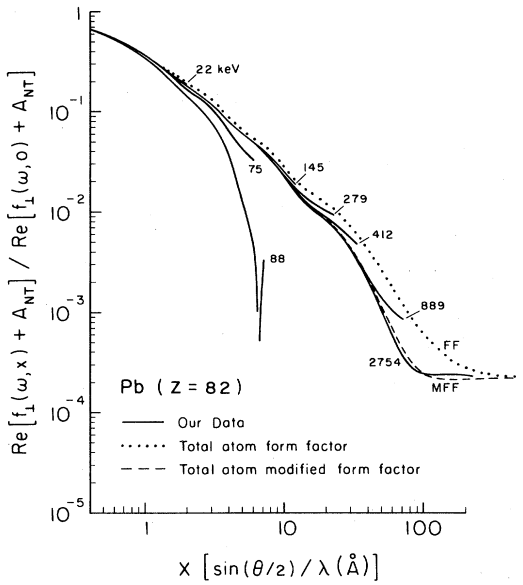

FIG. 4. Same as Fig. 3, but for Pb. Solid curves (——) are our numerical data, the dotted curve (· · · ·) is the relativistic form-factor prediction, and the dashed curve (— — —) is the modified form-factor prediction. The nuclear Thomson amplitude is responsible for the back-angle flattening at high energy.

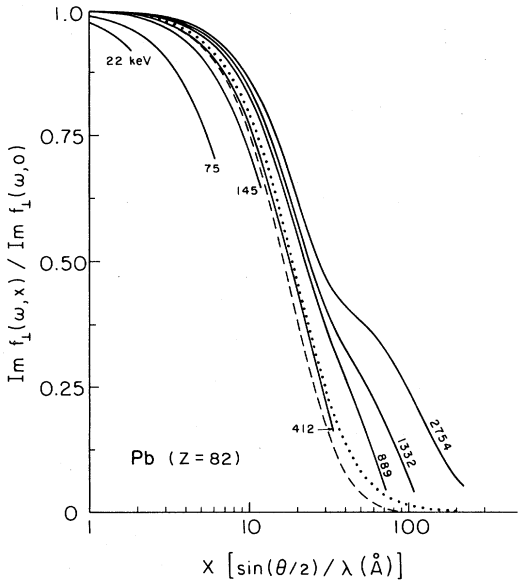

FIG. 6. Same as Fig. 5, but for Pb. Solid curves (——) are our numerical data, the dotted curve (· · · ·) is the K-shell relativistic form factor, and the dashed curve (— — —) is the K-shell modified form factor.

as is seen in Fig. 4 where we show the same comparisons for Pb. In this case we have added the nuclear Thomson amplitude, so that the curve goes to a constant for $x \gtrsim 90$ Å^{-1}. The form factor (dotted line) seriously overestimates our data (solid curves), even for fairly small q. What we are showing is a relativistic form factor, i.e., the Fourier transform of the relativistic charge distribution. As has been pointed out,[2] a *nonrelativistic* form factor is in fact considerably more satisfactory up to $x=10$. Except at 88 keV the modified form factor well represents our data

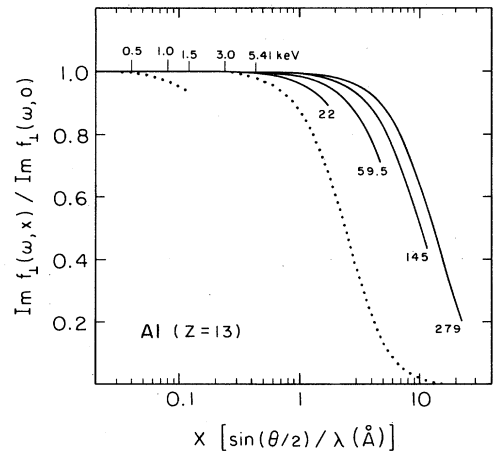

FIG. 5. Momentum dependence of the imaginary perpendicular amplitude normalized to the corresponding forward amplitude $[\mathrm{Im}f_\perp(\omega,q)]/[\mathrm{Im}f_\perp(\omega,q=0)] \equiv f''(\omega,q)/f''(\omega,q=0)$, as in Fig. 3, for Al. Solid curves (——) are our numerical data, dotted curves (· · · ·) the subshell form-factor scheme (see text), *not* the total atom form factor which would drop even more rapidly.

when $x \lesssim 20$ Å^{-1} for all ω, or when $\theta \lesssim 100°$ for all ω. The calculated amplitudes systematically stay above this common curve at back angles, showing a further dependence on ω as well as q, for high energies at back angles giving results which are intermediate between the form factor and modified-form-factor predictions. The perpendicular amplitude from lead at 88 keV (above but extremely close to threshold) changes sign at 143° because the K-shell contribution has changed sign and, although small, is nearly q independent: At back angles it can cancel the contribution from higher shells which is decreasing with q.

Near threshold then, it is clear that the assumption of form-factor q dependence can be incorrect for any atom. The assumption also generally fails for high-Z elements where, however, the form factor may be replaced by the modified-form factor for moderate q's.

A form-factor q dependence has also been assumed[30] for $\mathrm{Im}f_\perp \equiv f''$. In Fig. 5 for Al and Fig. 6 for Pb we show the q dependence of $\mathrm{Im}f_\perp(\omega,q)/\mathrm{Im}f_\perp(\omega,0)$ for various energies. In Fig. 5 we also show for 1.5 and 279 keV the form factor-based scheme suggested in Ref. 30,

$$f''_\perp(\omega,q) = \sum_j f''_{j,\perp}(\omega,0) f^{ff}_j(q)/f^{ff}_j(0) \,, \tag{8}$$

where the sum runs over all subshells j, $f''_{j,\perp}(\omega,0)$ is the forward imaginary amplitude from the jth shell, and $f^{ff}{}_j(q)$ is the form factor for the jth shell. (Note this prediction is energy dependent; the total atom form factor, not shown, would drop even more rapidly.) We see that in fact the imaginary scattering amplitude is less q dependent than any form-factor prescription. Below 59.5 keV, our data can be well fitted by a two-term multipole series

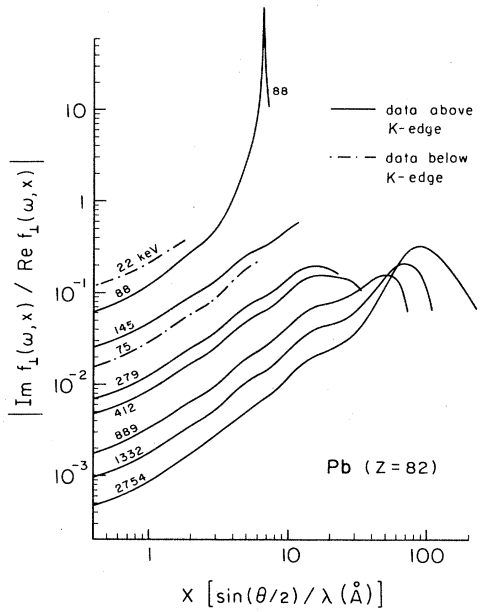

FIG. 7. Ratio of real and imaginary perpendicular amplitudes $[\mathrm{Im}f_\perp(\omega,q)]/[\mathrm{Re}f_\perp(\omega,q)]$ for Pb as in Fig. 3.

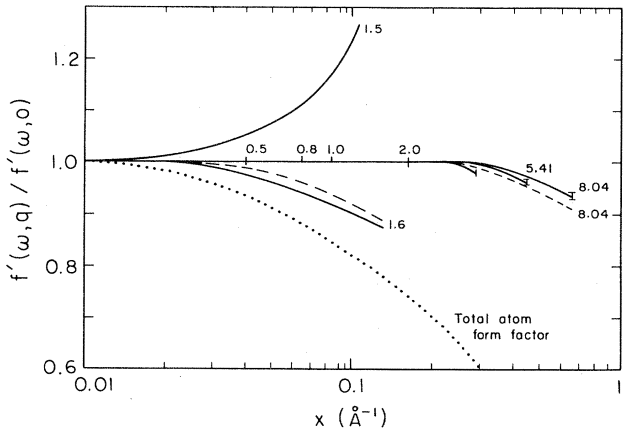

FIG. 8. Momentum dependence of the real perpendicular anomalous amplitude $f_\perp'(\omega,q)$ for Al, normalized to the corresponding forward value $[f_\perp'(\omega,q)]/[f_\perp'(\omega,0)]$, as in Figs. 3 and 5. Solid curves (——) are our numerical data, dashed curves (— — —) represent a subshell form-factor scheme like that of Eq. (8), and the dotted curve (· · · ·) is the total atom form factor.

$f_D''+f_Q''\cos\theta$ (see Ref. 18) forced to fit at 0° and 180°, while at higher energies more multipoles are needed. In Fig. 6 for Pb we display the K-shell form factor and K-shell modified form factor along with our data. With increasing energy our data (always less q dependent than total atom form factors) moves from more to less q dependent than K-shell modified form factor and form factor. For both Al and Pb, the q dependence of $\mathrm{Im}f_\perp$ decreases as the photon energy increases; at back angles the amplitudes continue to drop. On crossing the bound-pair creation threshold new structure appears in $\mathrm{Im}f_\perp$ around 90°, but it can be expected that other amplitudes probably dominate the Rayleigh contribution to elastic scattering at large q just as they do at forward angles.

The weaker q dependence of the imaginary parts of the amplitudes has the consequence that, although real forward amplitudes are much larger than the imaginary forward amplitudes in the circumstances we have considered, at larger q the imaginary parts may become comparable to the real parts. In Fig. 7 we show the q dependence of the ratio $\mathrm{Im}f_\perp(\omega,q)/\mathrm{Re}f_\perp(\omega,q)$ (note that forward amplitudes are not factored out) for various photon energies. Even excepting the 88-keV data, where $\mathrm{Re}f_\perp$ vanish at a particular q, in our data the ratio is as large as 50% and generally reaches more than 10% at intermediate angles.

The dispersion relations Eq. (5) for the scattering amplitude in the form usually used do not involve $\mathrm{Re}f$, but rather[15,17]

$$f'\equiv\mathrm{Re}\left[f(\omega)-\lim_{\omega\to\infty}f(\omega)\right],$$

which then defines the real part of the anomalous scattering factor f'. However, in the literature[6,11–14] f' is not usually referenced to the high-energy limit, as defined above in the forward scattering case, but rather is taken to be the same as

$$(\tilde{f}')=\mathrm{Re}f(\omega,q)-f^{ff}(q)\ . \tag{9}$$

This is only appropriate for low-Z elements and low q. (Note that the correct q dependence of the full amplitude in the high-energy limit is not known, though it has been obtained for the Coulomb K shell.[10]) In other circumstances the study of the q dependence of $\tilde{f}'$ is not particularly instructive. In light-Z elements the differences from form factor are sufficiently small that $\tilde{f}'$ rapidly becomes unimportant within the precision of our data. In high-Z elements the difference from form factor is always large and the q dependence of $\tilde{f}'$ is similar to that of $\mathrm{Re}f$ itself. We show in Fig. 8 the q dependence of $\tilde{f}'$ for Al at small q, where $\tilde{f}'\simeq f'$. Under these circumstances f' is nearly q independent, not at all like the form factor, and within the accuracy of the data behaves similarly to f''. This q independence is of some importance for the behavior of f in the near threshold region.

Beginning in the hard x-ray regime the simple relation between parallel and perpendicular amplitudes,

$$f_{||}=f_\perp\cos\theta\ , \tag{10}$$

begins to break down.[9,10,18] The amplitude $f_{||}$ continues to change sign as the general behavior of Eq. (2) requires, but at increasingly forward angles. To see the consequences for cross sections we show in Fig. (9) the ratio

$$\frac{\frac{1}{2}(|f_\perp\cos\theta|^2+|f_\perp|^2)}{\frac{1}{2}(|f_{||}|^2+|f_\perp|^2)}\equiv\frac{\cos^2\theta+1}{|f_{||}/f_\perp|^2+1}\ . \tag{11}$$

The error at some angles due to the use of Eq. (11) increases with Z for fixed energy, as well as growing with energy; for Al at 22 keV it is only 0.2%, while for Pb at 145 keV it is 5%. By the MeV range the effect has

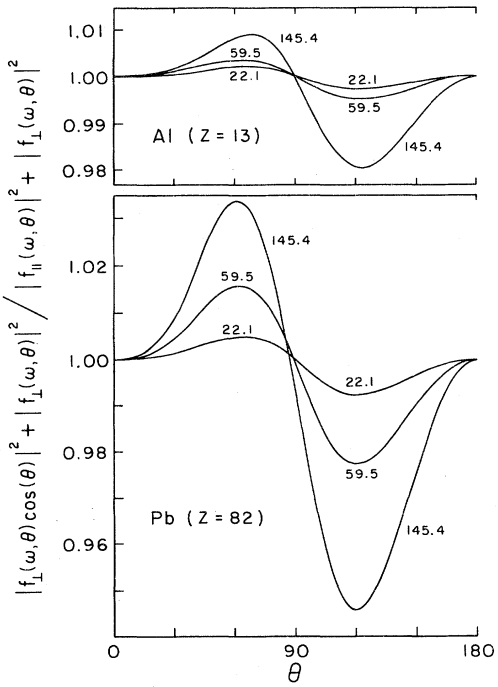

FIG. 9. Error in differential cross section due to use of relation $f_{||}=f_\perp\cos\theta$. The ratio of $\frac{1}{2}(|f_\perp|^2+|f_{||}|^2)$ with $f_{||}$ obtained from the relation, to that obtained using numerical results for both $f_{||}$ and $f_\perp$, is shown for Al and Pb at 22.1, 59.5, and 145.5 keV.

reached 30% (though of course at such energy large angle amplitudes are small).

We could also examine the q dependence of

$$\left[\frac{d\sigma}{d\Omega}(\omega,q)\right] \Big/ \left[\frac{d\sigma}{d\Omega}(\omega,0)\right] .$$

Qualitatively, the results are similar to those for Ref already shown. For Pb the modified-form-factor prediction, $|f^{\mathrm{MFF}}+A^{\mathrm{NT}}|^2$, is in good agreement with our data for $\theta \lesssim 100°$ at all energies and also at all angles for lower energies not too near threshold. Serious errors can result if instead of the MFF the form-factor approximation is used.

ACKNOWLEDGMENTS

The authors gratefully acknowledge fruitful discussions with Dr. Lynn Kissel, Dr. S. C. Roy, Dr. M. Gavrila, Dr. I. J. Feng, and M. S. Wang. Our data was computed from the program ENT, written by Dr. Kissel and slightly modified by one of us (J.P.). This work was supported in part by Lawrence Livermore National Laboratory subcontract No. 5342901 and National Science Foundation Grant No. PHY-81-20785.

[1]Lynn Kissel, R. H. Pratt, and S. C. Roy, Phys. Rev. A 22, 1970 (1980).

[2]S. C. Roy, Lynn Kissel, and R. H. Pratt, Phys. Rev. A 27, 285 (1983).

[3]G. E. Brown, R. E. Peierls, and J. B. Woodward, Proc. R. Soc. London, Ser. A 327, 51 (1954); S. Brenner, G. E. Brown, and J. B. Woodward, *ibid.* 227, 59 (1954); G. E. Brown and D. F. Mayers, *ibid.* 234, 387 (1955); 242, 89 (1957).

[4]W. R. Johnson and F. D. Feiock, Phys. Rev. 168, 1 (1968).

[5]W. R. Johnson and K. T. Cheng, Phys. Rev. A 13, 692 (1976).

[6]Don T. Cromer and David A. Liberman, J. Chem. Phys. 53, 1891 (1970); Acta Crystallogr. Sect. A 37, 267 (1981). In the following papers, Jensen discussed extension of this work, but in his second paper concluded that a better result was not available: M. S. Jensen, Phys. Lett. 74A, 41 (1979) and J. Phys. B 13, 4337 (1980).

[7]B. L. Henke, P. Lee, T. J. Tanaka, R. L. Shinabukuro, and B. K. Fujikawa, At. Data Nucl. Data Tables 27, 1 (1982).

[8]M. Gavrila, Phys. Rev. 163, 147 (1967).

[9]M. Gavrila and A. Costescu, Phys. Rev. A 2, 1752 (1970); 4, 1688 (1971).

[10]V. Florescu and M. Gavrila, Phys. Rev. A 14, 211 (1976).

[11]H. Hönl, Z. Phys. 81, 1 (1933); Ann. Phys. (Leipzig) 18, 625 (1933).

[12]R. W. James, *The Crystalline State,* edited by L. Bragg (Bell, London, 1968), Vol. II.

[13]L. G. Parratt and C. F. Hempstead, Phys. Rev. 94, 1593 (1954).

[14]*Anomalous Scattering,* edited by S. Ramaseshan and S. C. Abrahams (Munksgaard, Copenhagen, 1975), see especially S. Ramaseshan *et al.* for a partial review.

[15]M. Gell-Mann, M. L. Goldberger, and W. Thirring, Phys. Rev. 95, 1612 (1954); M. L. Goldberger, *ibid.* 97, 508 (1955); J. S. Toll, *ibid.* 104, 1760 (1958); T. Erber, Ann. Phys. (N.Y.) 6, 319 (1959).

[16]W. Zachariasen, *Theory of X-Ray Diffraction in Crystals* (Wiley, New York, 1945), pp. 90—96, especially Eq. (33).

[17]M. L. Goldberger and F. E. Low, Phys. Rev. 176, 1778 (1968).

[18]H. Wagenfeld, in *Anomalous Scattering,* Ref. 14, p. 13.

[19]Ramesh Narayn and S. Ramaseshan, Acta. Crystallogr. Sect. A 37, 636 (1981).

[20]G. Albanese, A. Deriu, and C. Ghezyi, Nuovo Cimento B 51, 3131 (1979).

[21]The relative phase of real and imaginary parts used in anomalous dispersion literature (Refs. 11—14) differs by a sign from that used in scattering literature (Refs. 1—9 and 14), with the imaginary amplitudes taken as positive in both cases.

[22]W. Franz, Z. Phys. 95, 652 (1935); 98, 314 (1935).

[23]Binding energies used here are from our relativistic self-consistent central-potential calculation of Ref. 1, not from experiment.

[24]J. S. Levinger, Phys. Rev. 87, 656 (1952).

[25]D. C. Creagh, Phys. Lett. 77A, 129 (1980); D. C. Creagh, Austr. J. Phys. 28, 543 (1975).

[26]W. Sommerfeld, *Optics* (Academic, New York, 1954).

[27]A. I. Akhiezer and V. B. Berestetskii, *Quantum Electrodynamics* (Interscience, New York, 1965), p. 492.

[28]M. Gavrila (private communication).

[29]R. H. Pratt, Phys. Rev. 117, 101 (1960).

[30]D. H. Templeton, in *International Tables for X-Ray Crystallography,* 2nd ed. (Kynoch, Birmingham, England, 1968), Vol. III, p. 213.